A network model of the coupling of ion channels with secondary messenger in cell signalling

Franck Plouraboué, Henri Atlan [*] , Gérard Weisbuch and Jean-Pierre Nadal

Laboratoire de Physique Statistique [+]
Ecole Normale Supérieure
24, rue Lhomond - 75231 Paris Cedex 05 France

Abstract

We demonstrate that formal neural networks techniques allow to build the simplest models compatible with a limited but systematic set of experimental data. The experimental system under study is the growth of mouse macrophage like cell lines under the combined influence of two ion channels, the growth factor receptor and adenylate cyclase. We conclude that 3 components out of 4 can be described by linear multithreshold automata. The remaining component behavior being non-monotonous necessitate the introduction of a fifth hidden variable, or of non-linear interactions.

P.A.C.S.:
87.10 General, theoretical and mathematical biophysics
87.25 Cellular biophysics
Short title: A network model of the coupling of ion channels

Preprint L.P.S. 363, February 1992
Appeared in Network: Computation in Neural Systems Volume 3, Number 4 (November 1992), pp. 393-406.

Introduction

A single cell viewed as a set of reacting chemical species is already a rather complex system. In fact the set of interacting genes and products in the cell was the object of one of the first modelisation of a living system in terms of boolean automata by S. Kauffman (1969) and by R. Thomas (1975). At the cell membrane level, biologically active compounds (growth factors, hormones, neurotransmitters, immunoreactive compounds, etc.) interact with specific receptor proteins. These "first messengers" interact with the receptor and induce a sequence of biochemical events which works like a channel of information transfer. At the end of the process, the cell performs the biological effect triggered by the signal: DNA synthesis and cell division by growth factors, nerve or muscle activity by neurotransmitters, turning on synthesis of given enzymes or activating given metabolic reactions by hormones. Following the interaction of first messengers with their receptors, systems of "second messengers" transfer the signal from the membrane to target molecular structures in the cytoplasm of the nucleus.

However, as discussed recently, rather than linear sequences of individual molecular events, the mechanisms involved must be analyzed as dynamic changes in the cellular state as in state machines (Lichstein & Atlan 1990). The number of second messengers is very small as compared to the number of structurally different receptors, each responsible specifically for a given biological effect. Therefore, in order to retain specificity at the level of the cytoplasmic or nuclear target, the second messenger must react in a complex manner with internalized or activated receptor associated membrane proteins which would serve as modulators of its activity. An example of a non specific activation of a receptor associated protein participating in a specific message may be found in observations on cell division induced by growth factors (Paris & Pouyssegur, 1986; Panet et al., 1986a,b; Pouyssegur et al., 1982; Berridge, 1986; Panet & Atlan, 1990, 1991). It was shown that growth factors induce an increase in both intracellular Ca^{++}, pH and

possibly Na^+, and all of these seem necessary to induce de novo DNA synthesis. Two ion transporters associated with the growth factor receptors (Na-H antiport and Na^+, K^+, Cl^- cotransport) seem to participate, at least as modulators, in the transfer of information by the second messenger. Thus, second messengers with their modulators, although not very specific by themselves, can be used in combinations by the cell to confer the specificity of the response. Evidence was presented (Rapp & Berridge, 1977) on coupling between cytoplasmic calcium and cAMP through common regulatory loops. Rapp & Berridge (1977) proposed mathematical models of instabilities leading to oscillations of the Ca^{++} and cAMP concentrations responsible for oscillatory behavior of several cellular properties. However, in general, oscillations are not the only possible outcome of such coupling. Sets of different steady-states can also be established.

More recently, a spatial-temporal model of cell activation has been proposed (Alkon & Rasmussen, 1988) taking into account multiple coupling (both in series and in parallel) between different components of Ca^+ $^+$ dependent second messenger, cAMP, ion channels and receptors. In most of these observations, the complexity of the interactions in the form of various couplings between different reactions, even for only one well-defined cellular function, often prevents a direct interpretation of available experimental results. System dynamics methods of analysis are necessary to help build up schemes of such interactions that would account for the observed cellular states. In fact, the state of a cell, as that of state machine (see Holcombe, 1982:66-71 for state machine representations of metabolic pathways), is the set of concentrations of its constitutive molecular species at every point in time and space co-ordinates. The change from one state to the other is governed by the chemical and transport kinetics of tens or hundreds of coupled reactions. Studies of such kinetics of relatively simple chemico-diffusional networks, involving not more than a few coupled reactions (Holcombe, 1982; Oster et al., 1973; Mickulecky, 1977; Atlan et al., 1979), have shown already that a change in the concentration of a compound somewhere in the metabolic network is likely to affect simultaneously the concentration of many other compounds elsewhere. Highly non-linear effects (excitatory or inhibitory) can be produced by feedback inhibition or autocatalytic loops, so that the classical idea of being able to modify one parameter at a time is generally wrong. The usual methods of quantitative analysis are those of reaction kinetics making use of sets of differential or partial differential equations. Network Thermodynamics (Oster & al., 1973) has been presented as a discrete representation, a priori more convenient for physicochemical couplings involving different energy domains. However, when confronted with actual experimental data on such coupled reactions obtained under in vivo conditions, e.g. of cell cultures, these methods are not of a great help because they need much more detailed data (binding constants, reaction rates, concentration changes, etc.) than what is available.

The purpose of this paper is to show that the techniques developed in learning by neural nets can be used to analyze sets of complex data from experiments on in vivo cellular systems. They will allow us to determine a set of interactions among receptors, ion transporters and second messengers that interact in the built up of a proliferative response to serum growth factors. The method is further called PAWN from the initials of the authors.

1. The experimental system

In a series of experiments, R. Panet, H. Atlan and co-workers studied the influence of ions transporters on the proliferation of different cell lines (mouse fibroblasts) and of human fibroblasts in culture (Panet & Atlan, 1990, 1991). In parallel, making use of cell lines of macrophages with mutants deficient in adenylate cyclase, A. Bourrit, H. Atlan et al. were able to show the influence of growth factor receptors, of adenylate cyclase, the enzyme implied in the synthesis of cAMP (a secondary messenger) and of two different transporters of Na^+ and K^+ ions, one ouabain sensitive (OS) and the other one bumetanide

sensitive (BS) (this means that they can be blocked respectively by ouabain or bumetanide). In other words, the two ion transporters and the enzyme play a role in the transduction of the primary message, the linking of the growth factor, into cell proliferation. But no simple linear scheme of interactions explains all the experimental results. Binary interactions seem to be sometimes positive, sometimes negative, and retro-action loops are likely. In order to elucidate the question, they did 12 independent experiments on the same system, i.e. the above-mentioned lines of macrophages. In each experiment but one, some of the four components of the system (growth factor receptor, adenylate cyclase, OS Na^+K^+ pump and BS $Na^+K^+Cl^-$ cotransporter were absent or inhibited (and thus clamped at null activity), and the activities of the non-clamped components were measured. .
One observes, for each component, from 2 to 4 (depending on the component) well distinct, reproducible, levels of activity. In the following, disregarding the precise values of the activities, we will only take into account the existence of different (and ordered) activity levels (Table 1), and propose the simplest possible model which is consistent with the experimental results.

Component:	I	II	III	IV
Exp. n°				
01.	0	1	2	3
02.	2	1	0	1
03.	3	0	1	2
04.	3	0	0	1
05.	2	0	1	0
06.	2	0	0	0
07.	1	1	2	0
08.	1	1	0	0
09.	0	0	1	1
10.	0	0	0	1
11.	0	1	2	3
12.	0	1	0	0

Table 1. Discretized activities of each component in the 12 experiments. Underlined zeros correspond to clamped activities.

Let us first comment the data of Table 1.
- Element **I** represents the bumetanide sensitive transporter. It can be clamped to zero by the presence of bumetanide in the culture, which block the activity of this Na/ K/ Cl co-transporter. The (measured) activities can take 4 possible discretised levels that we note 0, 1, 2 or 3 (corresponding resp. to experimental ranges: 0-2; 7; 12-13; 15-17; in μmol./10 min. for 10^6 cells).

- Element **II** represents the growth factor receptor activity which is set to 0 in the absence of the growth factor (serum deprived cells) and 1 in its presence.
- Element **III** is the adenine cyclase activity. This activity can have 3 possible levels, 0 , 1 or 2, (corresponding resp. to mutants deficient in the enzyme, to normal level in non mutants in the absence of growth factor or to activity stimulated by serum growth factors).
- Element **IV** is the oubain sensitive Na/K transporter, which can be clamped to 0 by the presence of oubain. The measured activities can take 4 possible levels 0, 1, 2 or 3 (corresponding resp. to experimental ranges: 0-2; 18-26; 33-35; 39-43; in μmol./10 min. for 10^6 cells).

The total number of independent experiments is in principle $16=2^4$, since each element can be either set free or clamped, but clamping all elements would bring no new information. Furthermore, since the authors were interested in the influence of growth factors on ionic transporters, the experiments where both would be clamped to zero were not done. This explains why the total number of experiments is limited to 12.

2. The PAWN method: theoretical framework

A simple theoretical framework compatible with the scarcity and precision of experimental results is that of network of threshold automata. Binary threshold automata are better known as formal neurons (Hertz et al. 1990). We here use a more general formalism, multithreshold automata (Thomas 1990). The "field" h_i acting on automaton i is defined by:

$$h_i(t) = \sum_{j \neq i} J_{ij}\ S_j(t) \tag{1}$$

where S_j (t) denotes the state of automaton j (j=1,...,N). The state S_i (t) of the multi-threshold automaton i having k_i possible states is computed according to the following set of rules:

$$\begin{array}{lll} \text{if} & h_i(t) < \Theta_i^0 & \text{then} \quad S_i(t+1) = 0 \\ \text{if} & \Theta_i^0 < h_i(t) < \Theta_i^1 & \text{then} \quad S_i(t+1) = 1 \\ & \ldots & \\ \text{if} & \Theta_i^{k_i-1} < h_i(t) & \text{then} \quad S_i(t+1) = k_i. \end{array} \tag{2}$$

In other words a multi-threshold automaton is a discrete monotonic function of the weighted sum of its inputs. The J_{ij} are the "weights" (or "couplings") that represent the influence of elements j on elements i.

In this framework, the interpretation of a set of experiment consists in building up the set of the multi-threshold automata specified by their interaction strength J_{ij} and their thresholds Θ_i^k. The interaction strength and the thresholds should be compatible with equations (2) when the automaton states are given the experimentally observed quantities written in Table 1 for the N=4 automata: these data tell us that 12 particular configurations of states $\{(S_i^\mu, i = 1, ..., N), \mu = 1, ..., 12\}$ are fixed points of the dynamics (2). The compatibility conditions are a set of inequalities which are explicitly given in the next sections.

In trying to solve for these inequalities, one should first note that they decouple in N (=4) independent sets, one for each automaton. The i^{th} set consists of p=8 inequalities (there are 12 experiments but for four of them the automaton is clamped to zero activity), for which the unknown are the thresholds of automaton i and the N-1 couplings J_{ij} giving the action of automata $j(\neq i)$ on i. In general, one expects for each set either no solution or an infinite number of solutions.

In the latter case, some additional criteria might be used to select a "best choice". The choice of the criteria is more or less arbitrary and is a matter of point of view. Ours is the search for the simplest model

consistent with the experimental data. Since the number of non-zero coupling is a measure of the complexity of the model, we minimize this number by setting to zero all couplings which sign is not specified by the inequalities. Once this is done, we optimize the couplings by maximizing the stability of the observed stationary configurations. The stability of the state of an automaton is defined by the distance of the field ***h*** to the thresholds. Maintaining a large distance to the threshold implies that small fluctuations of the field are unlikely to result in crossing a threshold, thus changing the state of the automaton. The stability of a set of configurations is maximum when the smallest stability among all the configurations is maximum. Figure 1 is a geometrical interpretation of the notion of stability. To compare stabilities among different set of couplings, these couplings have first to be normalised. We use the following normalisation:

$$J_{i1}^2 + J_{i2}^2 + J_{i3}^2 = 1 \qquad (3)$$

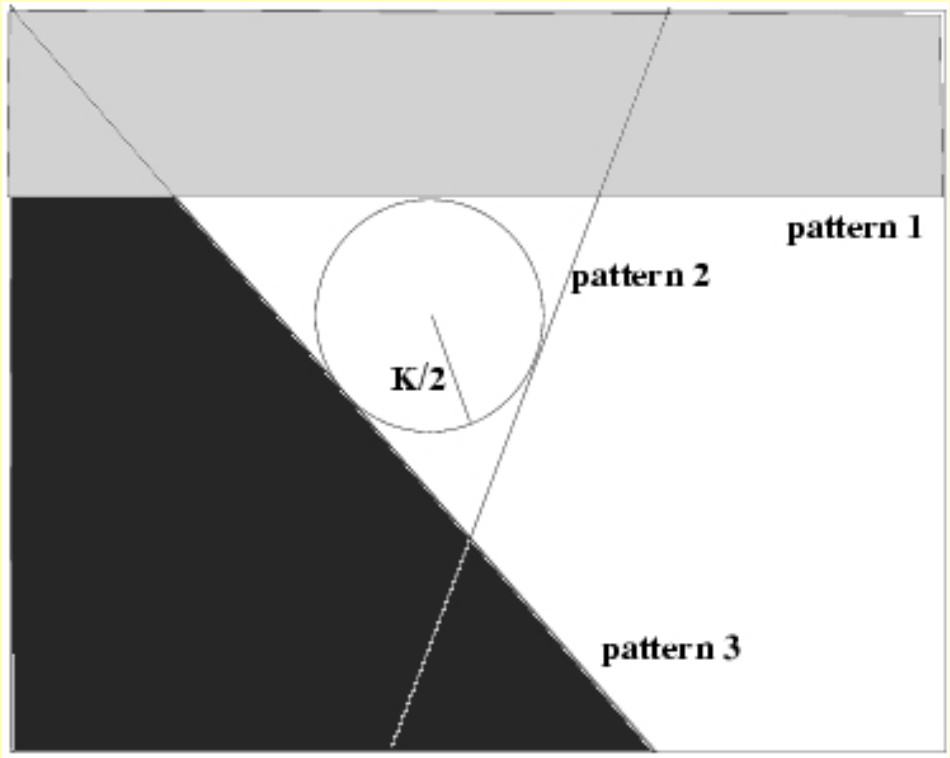

Figure 1. Geometrical representation of the stability ***K***. For a given automaton i, in the space of the J_{ij}, a field h_i for a given set of J_{ij} is represented by a point. Each configuration given by Table 1 is represented by one or two hyperplanes separating half-spaces where the inequality with respect to the threshold is true (unshaded regions) or false (the shaded regions). The components of the normal to the plane are the states S_j of the configuration. Solutions for the J_{ij} are in the unshaded region (when it exists; otherwise, there are no solutions). The stability of a solution is twice the distance of the field to nearest hyperplane. The maximum stability ***K*** is then twice the radius of the circle inscribed in the authorised region (this region might have more edges than the triangle represented on the figure in the case when there are more field inequalities).

To find the set of couplings that maximize stability one can use "learning" algorithms that have been derived for neural networks, such as the "minover" (Krauth and Mézard 1987) or the "adatron" (Anlauf and Biehl 1989) algorithms, variant of the well known perceptron algorithm (Minsky and Papert 1969), or the "active set approach" of Rujan (1991). In our case, due to the small number of automata, it turns out that all the solutions can be derived analytically (section 3). Another general remark is that only the couplings are unknown: the thresholds allowing maximum stability are fully determined once the couplings have been chosen - this point will be made clear in the next section.
When there is no solution - and this will be the case for automaton **I** -, one has to look for a more complicated model, and we will see (section 4) that there are several possibilities of similar complexities -

but with different biological interpretations.

3. PAWN method, step 1

3.1 Outline of results for automata II, III and IV

The main results, concerning the weights acting on automata **II**, **III** and **IV**, are given on Figure 2.

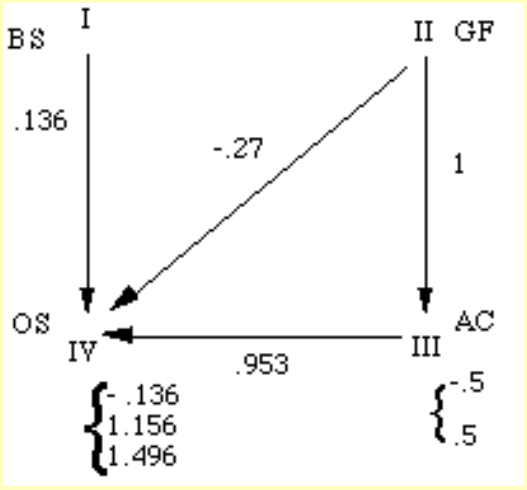

Figure 2. Couplings J_{ij} (along the edges) and thresholds Θ_i^k (after brackets) describing automata **II**, **III** and **IV**.

3.2 Detailed Solution

We first consider automata **II** and **III**. The state of automaton **II** is independent from the state of the other automata. When it is not maintained to 0, it is always 1. In some sense **II** is only an input to the network. Automaton **III** is either clamped to 0, or active at a level which only depends on the state of **II**. In the absence of **II**, automaton **III** is at level 1; it is strongly activated up to level 2 when **II** is active. The action of **II** on **III** is easily described in the above formalism by first writing the set of inequalities that have to be verified, applying the rules (2) for automaton **III**:

$$\Theta_3^0 < 0 < \Theta_3^1 < J_{32} \tag{4}$$

where we have already taken into account the absence of interaction from **I** and **IV** by setting the weights J_{31} and J_{34} to zero. Using the normalization (3) we have here $J_{32} = 1$. Then the thresholds are arbitrary values which allow to satisfy the inequalities (3). A particular solution is then the following choice of weights and thresholds:

$$J_{31} = J_{34} = 0 \quad J_{32} = 1 \quad \Theta_3^0 = -0.5 \quad \Theta_3^1 = 0.5 \tag{5}$$

Let us consider now automaton **IV**. The 8 inequalities that result from the data (Table 1) for automaton **IV** allow to position the fields with respect to the threshold as shown on Figure 3.

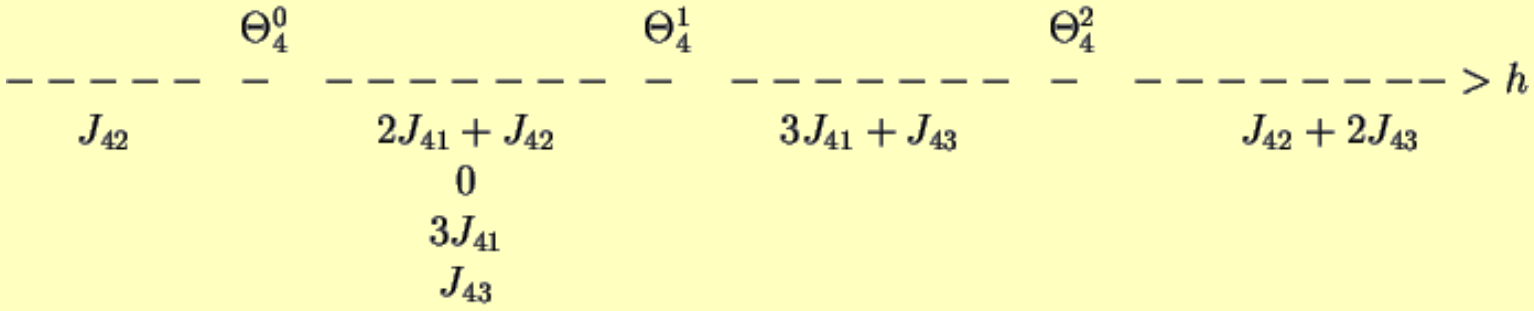

Figure 3. Respective positions of fields and thresholds for automaton **IV**.

By combining the field inequalities we obtain the following relations among the J_{4j} :

$$J_{42} < 0 \quad 0 < J_{41} \quad 0 < J_{43} \quad 3J_{41} < J_{42} + J_{43} \tag{6}$$

These conditions (6) give all the qualitative information that we need: there is an inhibitory action of automaton **II** on **IV**, and an excitatory action of **I** and **III** on **IV**. And the last inequality in (6) shows that the excitatory action of **III** is strong as compared to the actions of **II** and **I**.
To go beyond these qualitative results, we have to choose one particular solution. Normalization (eq.3) is applied. There is still an infinite number of solutions to the inequalities (6), but there exists a *unique* solution which maximizes the stability. A good stability is obtained when any two fields h_i^μ and h_i^ν which correspond to two different level of activity (say $S_i^\mu > S_i^\nu$), are as different as possible ($h_i^\mu - h_i^\nu$ is to be maximized). The best solution is the one which maximizes the smallest difference among all couples $S_i^\mu > S_i^\nu$ (and it is of course sufficient to consider only couples μ, ν with $S_i^\mu = S_i^\nu + 1$. In the case of automaton **IV**, among the 9 differences that can be written (see Figure 3), 6 can be shown to be implied by the 3 others. We then have to maximize

$$K \equiv \min\{-J_{42}, 2J_{41}, J_{42} + J_{43} - 3J_{41}\} \tag{7}$$

with the normalization (3). One can show, as indicated on Figure 1, that the solution is obtained when all the arguments in (7) are equal, leading to:

$$\begin{aligned} J_{41} &= 1/3\sqrt{6} \quad \sim 0.136 \\ J_{42} &= -2/3\sqrt{6} \quad \sim -0.272 \\ J_{43} &= 7/3\sqrt{6} \quad \sim 0.953 \end{aligned} \tag{8}$$

and the associated value of ***K*** is $2/3\sqrt{6} \sim 0.272$. The thresholds are set in the middle of the segment joining two closest fields:

$$\Theta_4^0 = -0.136 \quad \Theta_4^1 = 1.156 \quad \Theta_4^2 = 1.496 \tag{9}$$

3.3 Automaton I

The situation concerning the couplings to automaton **I** is different. Let us start from the fields diagram shown on Figure 4.This diagram shows inequalities that are contradictory: the two first inequalities on the first line imply that J_{14} should be negative and the two last ones that it should be positive. The action of automata **II**, **III** and **IV** on automaton **I** cannot be described by a unique linear threshold automaton and we have to complicate the model one degree further.

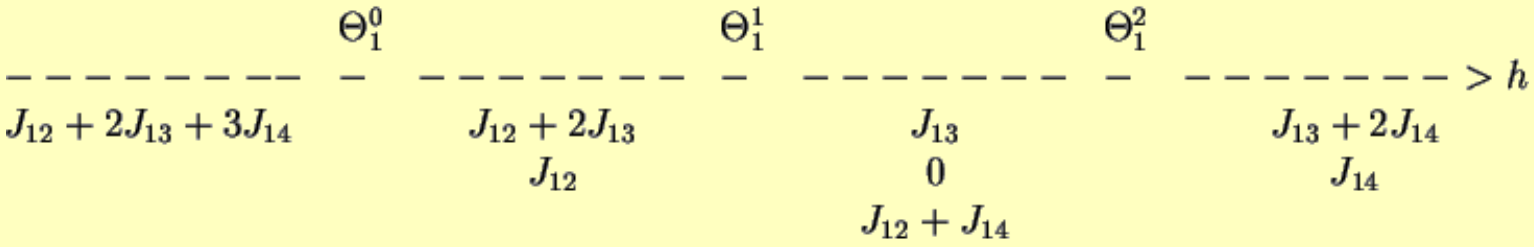

Figure 4. Respective positions of fields and thresholds for automaton **I**.

The non-monotonic action of **IV** on **I** reminds of the Equivalence Boolean function which is 1 when both arguments are 0 or 1, and 0 in the middle range when only one input is non-zero. The Equivalence function can be implemented by a non-linear threshold automaton, or by adding an extra linear automaton. These two simple solutions are discussed in the next sections.
In our case, it was easy to see that the linear model has no solution. This need not be the case for other problems, in particular if the number of automata is large. For such problems, one may use existing algorithms which allow precisely to know wether there exists a solution to the linear problem (Duda & Hart 1973, Nabutovsky & Domany 1991).

4. PAWN method, step 2

To go beyond we have to consider a slightly more complex model and, following our general strategy, we choose the least complex model which accounts for the data. In fact we will consider two possible generalizations of the preceding automata network model, which correspond to two different (but non exclusive) hypotheses: one is the occurrence of bimolecular interactions, and the other one is the existence of a fifth component. We will consider successively the two cases, leaving the discussion of the biological implications for section 6.

4.1. Higher order interactions

Let us add second order interactions to the linear interactions already taken into account. The field on automaton **I** now becomes:

$$h_1(t) = \sum_{j \neq 1} J_{1,j}\, S_j(t) + \sum_{1<j<k} J_{1,j,k}\, S_j(t) S_k(t) \tag{10}$$

We have thus three new couplings to compute, J_{123} , J_{124} , J_{134}. Writing the new inequalities and, after inspection, setting to zero all couplings for which the inequalities do not determine the sign, one has to solve:

$$0 = J_{13} \quad 0 = J_{123} \quad 0 = J_{124} \qquad 0 < J_{14}$$
$$0 < 2(J_{14} + J_{134}) \quad J_{12} < J_{14} + 2J_{134} \quad 3(J_{14} + 2J_{134}) < 0 \tag{11}$$

This inequalities imply that J_{134} should be negative, whereas J_{14} is positive: the direct coupling from **IV** to **I** is excitatory, whereas the combined interaction of **III** and **IV** on **I** is inhibitory. As for the case of automaton **IV**, we choose a particular solution, the solution with maximal stability. Here again this solution can be found analytically and one obtains:

$$J_{14} = -J_{12} = -2J_{134} = K = 2/3 \sim 0.66 \tag{12}$$

The results are summarized on Figure 5.

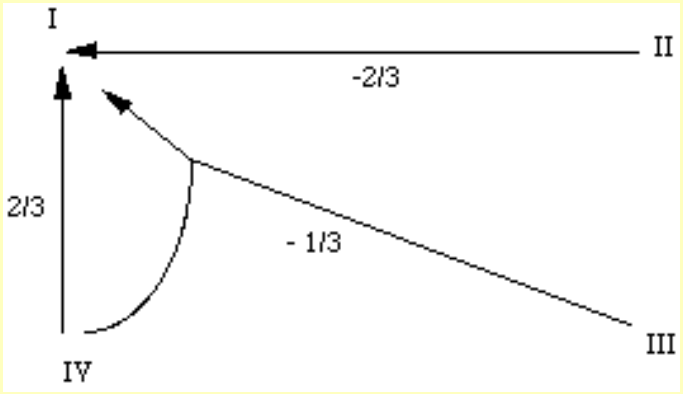

Figure 5. The non-linear solution for automaton **I**.

4.2. The hidden component.

Coming back to linear interactions, we now consider the possibility of the presence of a fifth automaton, **V**. To keep things simple, let us assume that this hidden unit may be either active (state 1) or inactive (state 0). We have then four additional couplings: the 3 couplings for the actions of automata **II**, **III** and **IV** on automaton **V**, and the coupling for the action of **V** on **I**. Of course, standard back-propagation algorithms (Le Cun 1985, Rumelhart et al 1986) could be used in this situation, but here again the solutions can be obtained analytically. Looking as before for the minimal solution, one first result is that only J_{54} and J_{15} are non zero. This was to be expected since only the correlation of the activities of **IV** and **I** matters here. Since the field received by **V** depends only on **IV**, there are only two formally equivalent possibilities. The negative influence of **IV** on **I** when **IV** level is low can be implemented either by:
- a positive action of **V** on **I**, active until the activity of **IV** reaches a threshold; in such a case $J_{54} < 0$ and $J_{15} > 0$, see Figure 6 a .
- a negative action of **V** on **I**, active after the activity of **IV** reaches the threshold; in such a case $J_{54} > 0$ and $J_{15} < 0$, see Figure 6 b .

The fact that these two possibilities are equivalent means the following. If one has a solution say for 6a, $(J_{54}, J_{1j}, \Theta_1^k, \Theta_5^0)$, then a solution $(J'_{54}, J'_{1j}, \Theta_1'^k, \Theta_5'^0)$ is derived for 6b as follows:

$$J'_{54} = -J_{54} \qquad J'_{1j} = J_{1j}\ (j = 1, ..., 4) \quad J'_{15} = -J_{15}$$
$$\Theta'^{k}_{1} = \Theta^{k}_{1} - J_{15} \quad (k = 0, 1, 2) \qquad \Theta'^{0}_{5} = -\Theta^{0}_{5} \tag{13}$$

Let us consider the first case (Figure 6 a). A simple examination of the system of equations shows that **V** must be inactive only when **I** is inactive. This leads the set of inequalities:

$$J_{54} < 0 \quad 3J_{14} < J_{15} \quad J_{12} < 0 < J_{14} \tag{14}$$

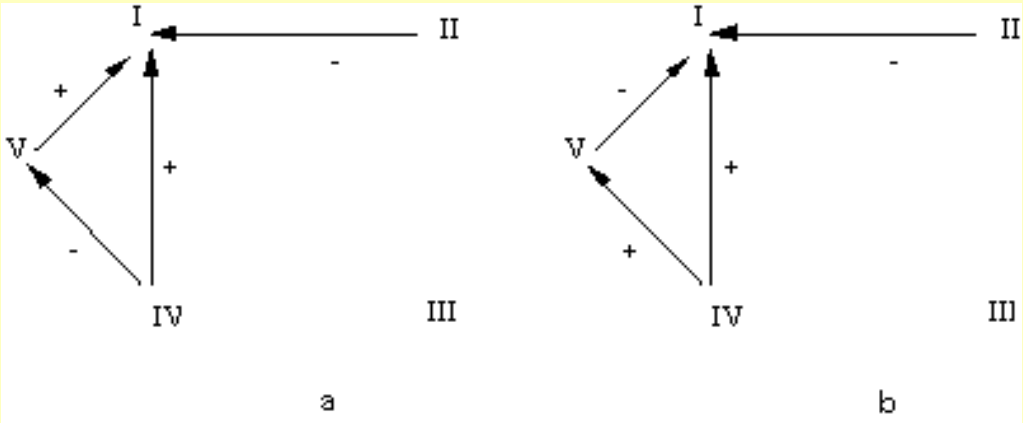

Figure 6. The solutions with a hidden unit for automaton **I**.

The optimal solution is here given by

$$J_{54} = -1 \quad J_{14} = -J_{12} = J_{15}/4 = K = 1/3\sqrt{2} \sim 0.235 \tag{15}$$

K being given by the normalization condition (3).

5. Dynamics

The model we have built takes into account all the data of Table 1. One can go a little further and explore the detailed network dynamics of the model. Starting with some initial conditions, one lets the network evolve, and note which fixed point, or periodic state, is reached. We already know that each configuration given on Table 1 is a fixed point: the couplings and thresholds have been computed for that. But there may be unwanted fixed points or limit cycles, and we are interested in the basin of attraction of each fixed point. Since we have a small network, an exhaustive exploration of the dynamics can be done. We will only give here the most significant results for the solution with a fifth component, as given in section 4, equation (13,15), together with the couplings given in section 3 for automata **II**, **III** and **IV**. Figure 7 shows the 4 iteration graphs obtained for fixed values of the states of automata **II** and **III** which are independent of the other automata. The only attractors are those observed in the experiments: optimizing the stability was probably the reason for the uniqueness of attractor.

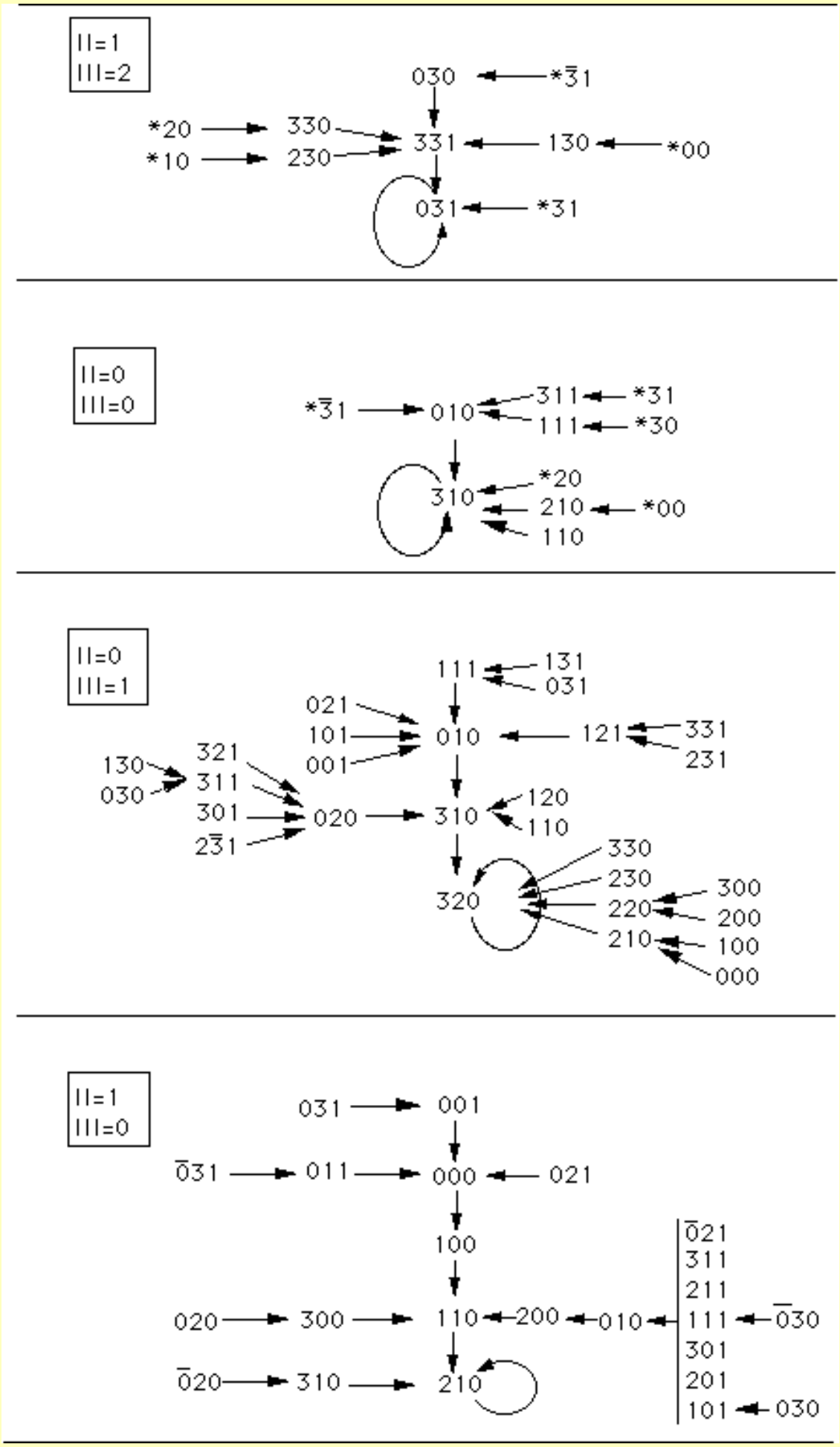

Figure 7. Iteration graphs for the solution with five linear automata when $J_{54} > 0$ and $J_{15} < 0$ (the network on Figure 6 b). The states of automata **II** and **III** which are independent of the other automata, are indicated at the

upper left corners of the 4 graphs. Each configuration of the network is then specified by the states of automata **I**, **IV** and **V** which are figured in a 3 digits representation. The first digit gives the state of automaton **I**, the second of automaton **IV** and the third of automaton **V**. The * symbol indicate any of the four states 0,1,2,3, and the bar above a digit means all digits except this one ($\bar{3}$ = {0,1,2}; $\bar{0}$ = {1,2,3}). The arrows indicate transitions from one configuration to the next one.

6. Biological interpretation

The method of analysis presented here allowed us to build up some of the simplest mathematical models that account for the observed experimental behavior. Most of the arbitrariness of the modelling is removed by the search for simplicity (cancelling of the connections, the sign of which is not fixed by the field inequalities) and for the most stable solution.

From a biological point of view, figs. 2, 5 and 6 show that the growth factors produce a direct inhibition of the two ion transporters accompanied by a much stronger indirect stimulation of the OS Na^+K^+ pump mediated by the activation of the adenylate cyclase dependent cAMP second messenger system. In addition, figs. 5 and 6 represent two different alternatives for a complex coupling pattern between the two ion transporters. In both cases, we are dealing with a double coupling: a direct, reciprocal positive one, whereby the activation of one of the transporters triggers the activation of the other and an indirect negative unidirectional one, whereby the activation of the OS Na^+K^+ pump produces an inhibition of the BS transporter.

- The former effect can be easily interpreted as the result of the changes in intracellular Na^+ concentrations produced by the activation or inhibition of each of the transporters. The OS transporter pumps out Na^+ from the cell whereas the BS transporter facilitates the entry of Na^+ into the cell. Both are very sensitive to changes in intracellular Na^+ concentration because of its normal very low value (of the order of 0.5 M). Therefore, any change in intracellular Na^+ produced by the activation of one of the transporters will produce a negative feedback by means of the activation of the other.

- The later effect can be produced by two different, non mutually exclusive mechanisms, which can be given different interpretations in terms of molecular interactions. In Figure 5, the assumed second order interaction means that the inhibitory effect of the OS pump on the BS transporter is dependent on the activation of the cAMP synthesis. Such an effect suggests a direct bimolecular reaction involving the two transporters. Contrary to the OS Na^+K^+ ATPase, the molecular structure responsible for the BS cotransport system has not yet been isolated. Therefore, the hypothesis of a direct interaction between the two (or three) molecular structures cannot be tested directly. On the other hand, the apparent difficulty in isolating and purifying a specific membrane protein proven to have the function of the BS transporter in intact membranes, may indicate that the function of this transporter cannot be easily separated from that of other membrane components. In Figure 6, the inhibitory effect of OS Na^+K^+ pump on the BS transporter is mediated by a so-called "hidden" component. In fact, based on data from different cellular systems, it is easy to guess what this component is likely to be. Studies on mouse and human fibroblasts (Panet & Atlan, 1990; Snyder et al, 1991a,b) have shown that some effects of growth factors on the BS transporter are mediated by their effect on the Inositol 3 Phosphate and Ca^{++} dependent second messenger system. Furthermore, a stimulating or inhibiting effect is observed depending on the physiological state of the cell (completely arrested or not) and on the nature of the Ca^{++} dependent second messenger pathway (Protein kinase C dependent or independent) activated by different growth factors tested separately.

In any case, the fact that the transporters and receptor system can be modelled by a set of 4 or 5 components does not imply that the set of chemicals involved in the regulation of the response is limited to

so few components. Each of the couplings indicated by an arrow is only a phenomenological representation which can be mediated by several reactions involving many chemicals. However, the modeling technique provides for a simple minimum model which allows to make sense of otherwise entangled uninterpretable data.

Acknowledgments. The Laboratoire de Physique Statistique is supported by CNRS (URA 1306). We acknowledge financial support from INSERM grant 879002.

References

Alkon, D. L. & Rasmussen, H. (1988), A spacial temporal model of cell activation. Science **239**, 998-1004.
Anlauf J. K. & Biehl M. 1989 "The adatron: an adaptative perceptron algorithm" Europhys. Lett. **10** 687
Atlan, H., Panet, R., Sidoroff, S., Salomon, J. & Weisbuch, G. (1979), Coupling of ionic transports and metabolic reactions in rabbit reticulocytes. Bond Graph Representation. J. Franklin Institute **308** (3), 297-308.
Berridge, M. (1986). In: *Calcium and the Cell* (Evered, D. & Whelan, J., eds) pp. 39-57, Chichester: Wiley.
Bourrit, A., Atlan, H., Fromer, I., Melmed, R. N. &Lichstein, D. (1985), Basic characterization of an ouabain-resistant, bumetadine-sensitive K+ carrier-mediated tranport system in J774.2 mousse macrophage-like cell line and in variants deficient in adelylate cyclase and cAMP-dependent protein kinase activities, Biochim. Biophys. Acta **817**, 85-94.
Duda R. O. and Hart P. E. (1973) *Pattern classification and scene analysis* (New-York, Wiley)
Holcombe, W. M. L. (1982). *Algebric Automata Theory* : Cambridge, England: Cambridge University Press
Hertz J., Krogh A. and Palmer D. (1990), *Introduction to the theory of Neural Computation* , Lectures notes in Santa Fe series on Complexity, Addison Wesley.
Kauffman S., (1969), Metabolic stability and epigenesis in randomly constructed genetic nets, J. Theo. Biology **22**, 437-467.
Krauth W. and Mézard M. 1987 " Learning algorithms with optimal stability in neural networks", J Phys A: Math Gen **20** L745
Le Cun Y. 1985 "A learning scheme for asymmetric threshold networks", in Cognitiva, (CESTA-AFCET Ed.), pp. 599-604
Lichstein, D. & Atlan, H. (1990), The "cellular state" : the way to regain specificity and diversity in hormone action, J. Theor. Biol **145**, 287- 294.
Mickulecky, D. C. (1977), A simple network thermodynamic method for series-parallel coupled flows, J. Theor. Biol. **69**, 511-541.
Nabutovsky D. and Domany E. (1991) "Learning the unlearnable", Neural Computation 605-616
Minsky M and Papert S, 1969 *Perceptrons* (MIT Press, Cambridge, MA)
Oster, G. F., Perelson, A. S. & Katchalsky, A. (1973), Network thermodynamics : dynamic modelling of biophysical systems, Q. Rev. Biophys. **6**(I), 1-134.
Panet, R., Amir, I. & Atlan, H. (1986a), Fibroblast growth factor induces a trasient net K+ influx carrier by the bumetadine-sensitive transporter in quiescent BALB/c 3T3 fibroblasts, Biochim. Biophys. Acta **859**, 1117-1121.
Panet, R., Snyder, D. & Atlan, H. (1986b), Amiloride added together with bumetadine completely blocks mouse 3T3 cell exit from GO/G1 phase entry into S-phase, Biochem. J. **239**, 745-750.
Panet, R. & Atlan, H. (1990), Bumetadine-sensitive Na+/K+/Cl- transporter is stimulated by Phorbol Ester and different mitogens in quiescent human skin fibroblasts, J. Cell. Physiol. **145**, 30-38.
Panet, R. & Atlan, H. (1991), Stimulation of Bumetadine-sensitive Na+/K+/Cl- Cotransport by different mitogens in synchronized human skin fibroblasts is essential for cell proliferation, J. Cell. Biol., in press.

Paris, S. & Pouyssegur, J. (1986),Growth factor activate the bumetadine-sensitive Na/K/Cl Cotransport in hamster fibroblasts, J. Biol. Chem. **261**(14), 6177-6183.
Pouyssegur, J., Chambard, J. C., Franchi, A., Paris, S. & Van Obberghen-Schilling, E. (1982), Growth factor activation of an amiloride-sensitive Na+/H+ exchange system in quiescent fibroblasts : coupling to ribosomal protein S6 phosphorilation, Proc. Natn. Acad. Sci U.S.A. **79**, 3935-3939.
Rapp, P. E. & Berridge, M. J. (1977), Oscillations in Calcium-Cyclic AMP control loops form the basis of pacemaker activity and other higgh frequency biological rhythms, J. Theor. Biol **66** , 497-525.
Rujan P. (1991), A fast method for calculating the perceptron with maximal stability, preprint
Rumelhart D.E., Hinton G.E., Williams R.J. 1986 "Learning internal representations by error propagation", in *Parallel Distributed Processing* , Rumelhart and McClelland Ed. (Bradford Books, Cambridge MA, 1986) Vol.1
Snyder, D., Markus, M., Atlan, H. & Panet, R. (1991a), The Phorbol ester TPA inhibits the stimulation of Bumetadine-sensitive Na+/K+/Cl- transporter by different mitogens in quiescent BALB/C 3T3 mouse fibroblasts , J. Cell. Physiol. **146**, 406-472.
Snyder, D., Atlan, H., Markus, M. & Panet, R. (1991b), Na+/K+/Cl- Cotransport is stimulated by a Ca++ -Calmoduline- mediated pathway in BALB/c 3T3 fibroblasts J. Cell. Physiol **149**, pp 497-502
Thomas R. (1975), *Kinetic Logic* , Lectures notes in Biomathematics vol. 29, Springer Verlag.
Thomas R. and D'Ari, R. (1990), *Biological Feedback* , Boca Raton Fl., CRC.
Weisbuch G., (1991) *Complex systems dynamics* , Lectures notes in Santa Fe series on Complexity, Addison Wesley.

---

[*] Service de Biophysique, Faculté de Médecine Broussais Hotel-Dieu, 15 rue de l'Ecole de Médecine, F- 75006 Paris; present address: Medical Biophysics, Hadassah University Hospital, Jerusalem, Israel.
[+] Laboratoire associé au C.N.R.S. (URA 1306) et aux Universités Paris VI et Paris VII